

# Supplementary material for Spin-to-orbital angular momentum conversion and spin-polarization filtering in electron beams

Ebrahim Karimi,<sup>1</sup> Lorenzo Marrucci,<sup>1,2</sup> Vincenzo Grillo,<sup>3,4</sup> and Enrico Santamato<sup>1</sup>

<sup>1</sup>*Dipartimento di Scienze Fisiche, Università di Napoli "Federico II",  
Complesso Universitario di Monte S. Angelo, 80126 Napoli, Italy*

<sup>2</sup>*CNR-SPIN, Complesso Universitario di Monte S. Angelo, 80126 Napoli, Italy*

<sup>3</sup>*CNR-Istituto Nanoscienze, Centro S3, Via G Campi 213/a, I-41125 Modena, Italy*

<sup>4</sup>*CNR-IMEM, Parco delle Scienze 37a, I-43100 Parma, Italy*

## GAUSSIAN ELECTRON BEAM IN HOMOGENEOUS WIEN FILTER

Let us consider an electron beam propagating in vacuum along the  $z$ -axis, subject to transverse and orthogonal electric and magnetic fields  $\mathbf{E}$  and  $\mathbf{B}$  lying in the  $xy$  plane. In this Section, we assume the two fields to be spatially uniform, as in standard Wien filters, but we will release this assumption later on. If the magnetic field direction makes an angle  $\alpha$  with the  $x$ -axis, we may write  $\mathbf{E} = E_0(\sin \alpha, -\cos \alpha, 0)$  and  $\mathbf{B} = B_0(\cos \alpha, \sin \alpha, 0)$ . As scalar and vector potentials, we may then take  $\Phi = -E_0(x \sin \alpha - y \cos \alpha)$  and  $\mathbf{A} = B_0(0, 0, y \cos \alpha - x \sin \alpha)$ , respectively. In the non-relativistic approximation and neglecting all Coulomb self-interaction effects (small charge density limit), the electron beam propagation is described by Pauli's equation

$$i\hbar\partial_t\tilde{\psi} = \left[ \frac{1}{2m}(-i\hbar\nabla - e\mathbf{A})^2 + e\Phi - \mathbf{B} \cdot \hat{\boldsymbol{\mu}} \right] \tilde{\psi} \quad (1)$$

where  $\tilde{\psi}$  is the spinorial two-component wave-function of the electron beam,  $e = -|e|$  and  $m$  are the electron charge and mass,  $\partial_t$  is the derivative with respect to the time variable  $t$ ,  $\hat{\boldsymbol{\mu}} = -\frac{1}{2}g\mu_B\hat{\boldsymbol{\sigma}}$  is the electron magnetic moment, with  $\mu_B = \hbar|e|\hbar/2m$  the Bohr's magneton,  $g \simeq 2$  the electron  $g$ -factor, and  $\hat{\boldsymbol{\sigma}} = (\hat{\sigma}_x, \hat{\sigma}_y, \hat{\sigma}_z)$  the Pauli matrix vector.

We seek a monochromatic paraxial-wave solution with average linear momentum  $p_c$  and average energy  $E_c = p_c^2/2m$  in the form  $\tilde{\psi}(x, y, z, t) = \exp[i(p_c z - E_c t)/\hbar]\tilde{u}(x, y, z)$ , where  $\tilde{u}(x, y, z)$  is taken to be a slow-varying envelope spinor field. Inserting this *ansatz* in Eq. (1) and neglecting small terms in the  $z$  derivatives of  $\tilde{u}$ , we obtain the paraxial Pauli equation

$$\partial_z\tilde{u} = \frac{i}{2k_c} \left( \nabla_{\perp}^2 - \frac{e^2}{\hbar^2}A^2 + \frac{2m}{\hbar^2}\mathbf{B} \cdot \hat{\boldsymbol{\mu}} \right) \tilde{u} \quad (2)$$

where  $\nabla_{\perp}^2 = \partial_x^2 + \partial_y^2$  is the Laplacian in the beam transverse plane and  $k_c = p_c/\hbar$  is the De Broglie wavevector along the beam axis. In deriving Eq. (2) we set  $E_0 = p_c B_0/m$ , so as to cancel out the average Lorentz force on the beam.

Equation (2) determines the evolution of the spinor field  $\tilde{u}$  along the axis  $z$ . This equation can be solved

analytically for the case of a gaussian input beam, as given by  $\tilde{u}(r, \phi, 0) = \tilde{a} \exp[-r^2/w_0^2]$  for  $z = 0$ , where  $w_0$  is the beam waist and  $\tilde{a} = (a_1, a_2)$  the input spinor, corresponding to an arbitrary spin superposition  $|\psi\rangle = a_1|\uparrow\rangle + a_2|\downarrow\rangle$ . A straightforward calculation shows that the solution is given by

$$\tilde{u}(r, \phi, z) = G(r, \phi, z)\hat{M}(z)\tilde{a} \quad (3)$$

where  $\hat{M}(z)$  is the matrix

$$\hat{M}(z) = \begin{pmatrix} \cos \frac{2\pi z}{\Lambda_1} & ie^{-i\alpha} \sin \frac{2\pi z}{\Lambda_1} \\ ie^{i\alpha} \sin \frac{2\pi z}{\Lambda_1} & \cos \frac{2\pi z}{\Lambda_1} \end{pmatrix} \quad (4)$$

where  $\Lambda_1 = (2\pi\hbar^2 k_c)/(mg\mu_B B_0)$  and the scalar gaussian factor  $G(r, \phi, z)$  is given by

$$G(r, \phi, z) = g_0(z)e^{ik_c r^2 \left( \frac{\cos^2(\alpha-\phi)}{2q_1(z)} + \frac{\sin^2(\alpha-\phi)}{2q_2(z)} \right)} \quad (5)$$

with

$$g_0(z) = \frac{\sqrt{\pi} z_R e^{-\frac{1}{2} \arctan\left(\frac{z}{z_R}\right)} e^{-\frac{1}{2} \arctan\left(\frac{\Lambda_2}{\pi z_R} \tan \frac{\pi z}{\Lambda_2}\right)}}{(z_R^2 + z^2)^{\frac{1}{4}} \left( \pi^2 z_R^2 \cos^2 \frac{\pi z}{\Lambda_2} + \Lambda_2^2 \sin^2 \frac{\pi z}{\Lambda_2} \right)^{\frac{1}{4}}} \quad (6)$$

$$q_1(z) = z - iz_R, \quad (7)$$

$$q_2(z) = \frac{\Lambda_2}{\pi} \left( \frac{\Lambda_2 \sin\left(\frac{\pi z}{\Lambda_2}\right) - i\pi z_R \cos\left(\frac{\pi z}{\Lambda_2}\right)}{\Lambda_2 \cos\left(\frac{\pi z}{\Lambda_2}\right) + i\pi z_R \sin\left(\frac{\pi z}{\Lambda_2}\right)} \right), \quad (8)$$

where  $z_R = \frac{1}{2}k_c w_0^2$  and  $\Lambda_2 = \frac{\pi\hbar k_c}{eB_0} = g\Lambda_1/4 \simeq \Lambda_1/2$ .

The matrix  $\hat{M}(z)$  given in Eq. (4) corresponds to Eq. 2 in the main paper and describes the magnetic-field-induced Larmor spin precession during propagation and the associated geometric phases discussed in the main paper. The precession length  $\Lambda_1$  corresponds to two full spin rotations.

In addition to the spin dynamics, from Eq. (8), we find that the wavefront complex curvature radius  $q_2(z)$  in the direction perpendicular to the magnetic field  $\mathbf{B}$  changes periodically with spatial period  $\Lambda_2$ . These oscillations correspond to the well known astigmatic lensing effect of the Wien filter.

## SPACE-VARIANT WIEN FILTER AND RAY-TRACING SIMULATIONS

In this Section, we consider “ $q$ -filter” field geometries with cylindrical symmetry, described by the following expression for the magnetic field (with the vector given in cartesian components):

$$\mathbf{B}(r, \phi, z) = B_0(r)(\cos \alpha(\phi), \sin \alpha(\phi), 0) \quad (9)$$

where the angle  $\alpha$  is now the following function of the azimuthal angle:

$$\alpha(r, \phi, z) = q\phi + \beta \quad (10)$$

where  $q$  is an integer and  $\beta$  a constant. As discussed in the main paper, such a field pattern must have a singularity of topological charge  $q$  at the beam axis  $r = 0$ . In particular, by imposing the vanishing of the field divergence, we find that the radial factor  $B_0(r) \sim r^{-q}$ , i.e., the field vanishes on the axis for negative values of  $q$ , while it diverges for positive values of  $q$ . In the latter case, there must be a field source on the axis. The electric field will be taken to have an identical pattern, except for a local  $\pi/2$  rotation, so as to balance everywhere the Lorentz force. We are particularly interested in the negative  $q$  geometries, which do not require to have a field source at the beam axis. For example, the  $q = -1$  case corresponds to the standard quadrupole geometry, while  $q = -2$  corresponds to an hexapole one.

The electron propagation problem in such non-uniform field can only be solved approximately or numerically. A second-order geometrical optics solution is reported in Ref. [1], which includes also a detailed analysis of spin precession but without considering the geometric phase effect (as well as the magnetic dipole forces). This analysis shows that, to first order, a balanced Wien filter having quadrupole or hexapole geometry but vanishing dipole term (as in our  $q$ -filter) is already stigmatic, i.e. it preserves the cylindrical symmetry without need for further corrections. The only beam lensing or distortion effects enter as higher-order aberrations (i.e., the  $G$  term in Eq. (31) of Ref. [1]).

To further analyze the behavior of our  $q$ -filter, we have performed ray-tracing simulations of the electron propagation for a quadrupole geometry ( $q = -1$ ). The magnetic and electric fields have been calculated using COMSOL finite-elements simulation (www.comsol.com). The ray-tracing routines therein contained have been used to assess the shape of the beam at the exit of the filter starting from an input beam having 100 keV of energy that is shaped as a ring, with a radius  $r$  of 100  $\mu\text{m}$ . The magnetic field at  $r$  needed to obtain the tuning condition  $\delta = \pi$  is 3.5 mT, with a corresponding electric field of 575 kV/m. These are obtained in our geometry with an electrode potential difference of  $\approx 9$  kV and a magnetization of 135 A/mm. The fields need to be set to the design-values

with a precision of 1 part in  $10^4$ . The electron velocity to be used as initial conditions in the simulations must be obtained from a model of the fringe fields. For the simplest description of the input fringe fields, i.e. the so-called sharp cut-off fringing field (SCOFF) model, the transverse velocity components remain constant and nil, i.e.  $v_x = v_y = 0$ , while the  $z$ -component  $v_z(x, y)$  “just inside” the filter is given by the following expression:

$$v_z(x, y) = v_0 - \frac{e\Phi(x, y)}{mv_0} = v_0 - \frac{eA_z(x, y)}{m} \quad (11)$$

where  $v_0$  is the velocity outside the filter. This condition is derived from the conservation of energy and also ensures the conservation of the canonical momentum of the electrons entering the Wien filter and hence the conservation of their wavefront orientation. The results of

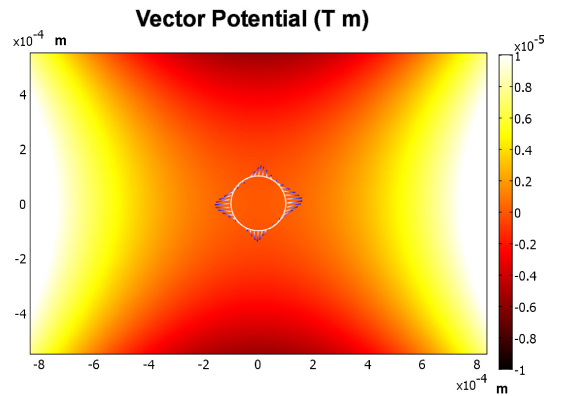


FIG. 1. Projection on the  $xy$  plane of the simulated trajectories of the electrons starting from a circle of radius  $r = 100$   $\mu\text{m}$ . The trajectories are shown with a color growing darker as  $z$  is increased.

ray-tracing simulations are reported in Fig. 2 of the main paper and in Fig. 1 of the present manuscript, which show how a circle of electron positions representative of the input beam becomes deformed during the propagation into a quadrupole-lobed shape, due to second- or higher-order aberrations. For optimizing the performances of our proposed device, in particular in the spin-polarization filter application, these aberrations should probably be compensated by additional electron optics (e.g., octupole electrostatic lenses). Nevertheless, even for no aberration compensation, the vortex effect giving rise to the radial separation of the two spin components discussed in the spin-polarization application is expected to be preserved, owing to its topological stability.

## MAGNETIC DIPOLE FORCES AND ANGULAR MOMENTUM

We now evaluate the effects of the force associated with the magnetic dipole of the electrons in the magnetic field gradient of the Wien filter. This is the force used in Stern-Gerlach experiments and the only spin-dependent force acting on the electrons, so it is important to assess its effects in detail. At any given point inside the filter, assuming that the magnetic dipole of the electron is  $\boldsymbol{\mu} = -g\mu_B\mathbf{S}$ , where  $\mathbf{S}$  is the corresponding spin vector, the associated magnetic force is

$$\mathbf{F} = \nabla(\boldsymbol{\mu} \cdot \mathbf{B}) \quad (12)$$

where the gradient must be taken while keeping  $\boldsymbol{\mu}$  constant, i.e. acting only on the magnetic field coordinates. For our classical estimate, the magnetic dipole evolution can be described by the precession equation

$$\frac{d\boldsymbol{\mu}}{dt} = \frac{g|e|\hbar}{2m} \mathbf{B} \times \boldsymbol{\mu} \quad (13)$$

Assuming a starting magnetic moment parallel to the  $z$  axis, the magnetic dipole will rotate around the local magnetic field direction. In the approximation in which aberrations are neglected, each electron travels along a parallel ray with constant transverse coordinates, and hence sees a uniform magnetic field, given by Eq. (9). Therefore, the magnetic dipole at any given point inside the filter will be given by the following expression:

$$\boldsymbol{\mu}(r, \phi, z) = \mu_B [-\sin \delta(r, z) \sin \alpha(\phi), \sin \delta(r, z) \cos \alpha(\phi), \cos \delta(r, z)] \quad (14)$$

where  $\delta(r, z)$  is the total spin precession angle at  $z$ , for a trajectory at radius  $r$ . Taking the scalar product between  $\boldsymbol{\mu}$  and  $\mathbf{B}$  and then the gradient with respect to the coordinates of  $\mathbf{B}$  only, we find that the magnetic dipole force is only directed along the azimuthal direction and given by

$$\mathbf{F} = \hat{\phi} q \frac{\mu_B B_0(r)}{r} \sin \delta(r, z) \quad (15)$$

where  $\hat{\phi}$  denotes the unit vector along the azimuthal direction and we have used Eq. (10) for taking the  $\phi$  derivative.

Equation (15) can be used for two purposes. First, we can verify that the ray deflection inside the Wien filter due to this force is negligible. Indeed, integrating the force in the time  $T$  needed for a full  $\pi$  rotation of the spin (or spin flip), we obtain the overall momentum change

$$\begin{aligned} \Delta p_\phi &= \int_0^T F_\phi(t) dt = \int_0^\pi F_\phi(\delta) \left( \frac{d\delta}{dt} \right)^{-1} d\delta \\ &= \frac{2m}{g|e|B_0} \int_0^\pi F_\phi(\delta) d\delta = \frac{2q\hbar}{gr} \end{aligned} \quad (16)$$

We can see from this equation that the momentum variation is of the same order as the quantum uncertainty in momentum of the electron wavefunction, taking into account that the position uncertainty is of the same order of the beam size  $r$  (as it is also expected based on Bohr impossibility theorem, as discussed further below). This momentum change produces negligible effects in the electron propagation across the filter, although it instead becomes relevant in the far field. Indeed, it is precisely this force that produces the orbital angular momentum change at the basis of our spin selection. Indeed, we will now show that the torque associated with the magnetic dipole force is that responsible for the OAM change of the electrons. The  $z$ -component torque of this force is given by

$$\begin{aligned} M_z &= (\mathbf{r} \times \mathbf{F})_z = q\mu_B B_0(r) \sin \delta = q(\boldsymbol{\mu} \times \mathbf{B})_z \\ &= -q \frac{dS_z}{dt} \end{aligned} \quad (17)$$

where  $S_z$  is the  $z$  component of the electron spin angular momentum  $\mathbf{S}$ . Since this torque acts on the OAM of the electrons  $L_z$ , we find the following angular momentum coupling law:

$$\frac{dL_z}{dt} = -q \frac{dS_z}{dt} \quad (18)$$

Once integrated for the entire flight time, corresponding to a full spin flip, this coupling law returns the same result reported in the main paper for the OAM variation induced by the spin flip.

This correspondence proves that the effect, and the only effect, of the magnetic dipole force acting on the electrons is the change of OAM already considered by including the geometric phase shift in the wavefunction emerging from the filter. Therefore, the only significant effect of this force appears in the far field and is exactly the effect that we propose to utilize to separate electrons according to their spin.

## FRINGE FIELD EFFECTS

The actual fringe fields depend on the electrodes and magnetic poles geometry. It is however safe to assume that the fringe fields extend only for a longitudinal distance along the  $z$  axis that is comparable to the transverse aperture of the Wien filter, and therefore much smaller than the filter length, in the large length-to-gap ratio limit. Moreover, the transverse components of the fringe fields can be taken to have exactly the same multipolar geometry as the fields inside the Wien, and hence will give rise to similar effects both in lensing and spin precession. Their overall effect is therefore only to change the effective length of the filter. However, in addition there will also be a longitudinal  $z$  component that must be taken into account. In the lensing effect, only the  $z$

component of the electric field plays a role, by ensuring the validity of the condition (11). The  $z$  component of the magnetic fields does not affect the ray propagation, since it exerts a vanishing Lorentz force. However, the latter may affect the spin precession. If we assume that the input electrons have a spin parallel to the  $z$  axis, then the  $z$  component of the fringe magnetic field does nothing. However, the spin may be somewhat rotated away from the  $z$  axis by the transverse fringe magnetic field, and in this case the longitudinal component will induce some non-uniform precession around the  $z$  axis that may partly depolarize the beam. This effect will however be proportional to the time spent by the particles in the fringe field region, and hence will be negligible in the large length-to-gap ratio limit.

We may also consider the idealized limit of an extremely thin fringe field region in which the electric and magnetic fields vary rapidly from the vanishing values they have away from the Wien filter to the values they acquire well inside the filter, which then remain perfectly constant. This is the SCOFF limit mentioned above. In particular, in the SCOFF limit the vector potential  $\mathbf{A}$  must go from zero to the value  $\mathbf{A} = [0, 0, A_z(x, y)]$  describing the multipolar magnetic field inside the filter. This rapid transition does not give rise to any magnetic field, because it is curl-free. Therefore, the SCOFF limit has vanishing magnetic fringe fields and therefore absolutely no effect on the spin, nor on the lensing behavior of the filter. On the other hand, in the SCOFF limit the electric potential must go from zero to the nonzero value  $\Phi(x, y)$  describing the multipolar electric field inside the filter. This in turn implies the presence of a very strong longitudinal electric fringe field that is responsible for the change of velocity given by Eq. (11). We stress that this idealized SCOFF description of the fringe fields needs not being realistic, but it is sufficient to identify the ineliminable effects that the fringe field impose to the electrons, and therefore the possible fundamental limitations that may arise from them.

### LAYOUT OF A SPIN-POLARIZED TEM MICROSCOPE

We report in Fig. 2 the sketch of a possible TEM microscope incorporating the proposed spin-polarization filter based on the  $q$ -filter. Such a device could be used to perform spin-sensitive TEM microscopy on magnetic materials or spintronic devices. It includes the four stages discussed in the main paper, i.e. (i) the fork hologram to set the initial OAM, (ii) the  $q$ -filter to couple OAM to spin, (iii) an imaging stage to go in the Fourier plane, (iv) an aperture to select a single spinorbit component, as well as the additional electron optics needed for imaging and collimating the beam. The input aperture of the system is defined by the fork hologram mask and has a

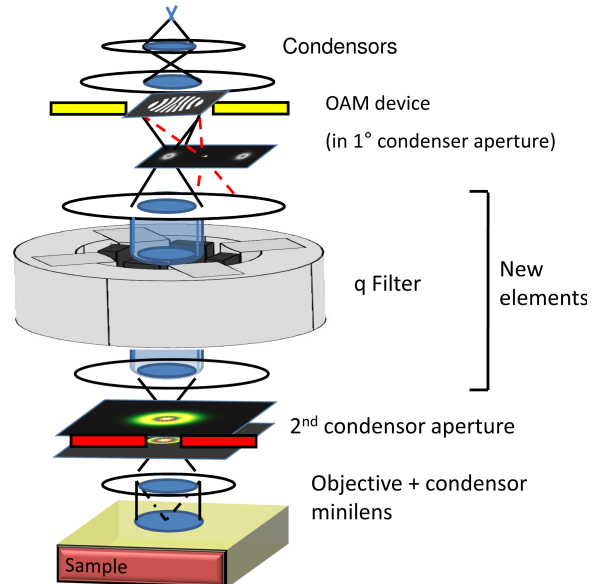


FIG. 2. Sketch of a possible TEM microscope incorporating the proposed spin-polarization filter based on the  $q$ -filter.

typical radius of few microns [2]. The output iris needed to select a single spin polarization can be set to a radius of few tens of microns, by carefully selecting the aperture plane position with respect to the focal plane. It will be presumably convenient to work slightly off focus to obtain larger beam waists without the need to introduce additional magnifying optics.

We note here in passing that in the new generation of TEM microscopes with aberration-corrected probe a larger number of lenses are available for beam control, and in particular a pair of hexapoles. It could be worth then exploring the possibility of using directly these lenses as an effective  $q$ -filter, without introducing additional optical elements. In this configuration, the magnetic hexapoles with opposite sign could be used to produce the polarization, while also compensating the introduced aberration. However stability issues might arise for large fields and the effect of fringing fields on the spin may also not be negligible, in this case, as the length-to-gap ratio would not be very large. Therefore, further analysis and simulations will be necessary in order to assess this possibility.

### THE ROLE OF ELECTRON DIFFRACTION

In our treatment we fully included the diffraction effects only in the free propagation (through a lensing system) taking place after the  $q$ -filter device. Indeed, this stage is where the correlation between OAM and radial profile develops and is then exploited for separating the different spin components. This free propagation, end-

ing in the far-field and giving rise to the beam profiles shown in Fig. 3 of the main paper, has been evaluated using a fully quantum mechanical treatment. The diffraction effects are obviously important in the propagation from near to far field, and in particular in determining the presence or absence of destructive interference effects at the vortex position that are essential in our proposed scheme.

One may wonder if we can legitimately ignore the diffraction effects in the other stages of our proposed setup. For the propagation through the  $q$ -filter, we could assess directly the role of diffraction in the case of homogeneous field, for which we have both the exact solution of Pauli's equation (including diffraction) and the classical trajectory solutions. We find that diffraction is only relevant if we look at the electron beam very close to a focal point, where its width becomes of the order of few nanometers. Away from the focus, the ensemble of classical trajectories reproduces perfectly well the quantum beam evolution. This result is not surprising, as in the  $q$ -filter all length scales are 8-9 orders of magnitude larger than the electron wavelength  $\lambda = 2\pi/k_e$ , which is of few picometers for energies of the order of 100 keV (typical of electron microscopes). Therefore, we may safely assume that diffraction can be ignored also in inhomogeneous  $q$ -filter geometries, as long as no focusing occurs inside the filter. Our classical ray-tracing simulations confirm that we avoid a focusing inside the  $q$ -filter. It should be also noted that in designing and analyzing electron-optics elements as those commonly used in electron microscopy, it is quite standard to ignore quantum effects and use classical ray tracing or geometrical optics.

The input and output apertures, being again about 7 orders of magnitude larger than the electron wavelength, will also give negligible diffraction effects (only some radial fringes extremely close to the aperture edges are expected, which should not affect the proper working of the proposed setup).

### VIOLATION OF BOHR'S "THEOREM"

As reported in Ref. [3], few years after the discovery of electron spin, several experiments were proposed (and sometimes attempted) aimed at separating electrons according to their spin, mainly by exploiting inhomogeneous magnetic fields acting on the magnetic dipole associated with it (similar to the Stern-Gerlach experiment). In 1929, Niels Bohr demonstrated a sort of "impossibility theorem" [3], stating that no Stern-Gerlach-like experiment (including Knauer's proposal, in which an electric field was used to balance the Lorentz force) could be used to separate electrons according to their spin by more than a small fraction of the beam transverse extension. This was related to the uncertainty principle and to the unavoidable orthogonal magnetic field accompanying

the required magnetic field gradient. A simple explanation of this result is that the spin magnetic moment vanishes in the classical limit  $\hbar \rightarrow 0$ , so all attempts at separating particles according to the magnetic-moment force occurring in a magnetic field gradient give rise to a vanishing separation in the classical limit, and hence a separation that is comparable to quantum uncertainty. Actually, this statement has been later proved not to be strictly valid (see, e.g., Refs. [4, 5]), although it remains extremely hard to overcome in practice.

Our approach is however fundamentally different from past attempts. Indeed, we exploit the quantum nature itself of the electrons to operate the spin separation (as such, our proposal bears some similarities with a very recently proposed scheme for spin-polarization in which electron diffraction is also exploited [6]). As we have seen, the magnetic dipole force in our device acts only in the azimuthal direction, which is not the direction along which we separate the electrons. The torque associated with this force imparts the OAM variation corresponding to the azimuthal geometric phase. However, at the exit of our Wien filter the electrons show no significant spatial separation according to the spin. It is then the subsequent free propagation and diffraction that acts to separate the electrons along the radial direction, which is not the direction of the main field gradient. In particular, an efficient radial separation is ensured by the presence of a vortex at the beam axis for one spin component and not for the other. In other words, we use the quantum wavy nature of the electrons to separate them according to the spin, and hence our method is not subject to Bohr's impossibility theorem. As a further argument, even in the classical Stern-Gerlach approach Bohr's theorem does not forbid the creation of spin-polarized components at the edges of the beam, so that by suitable aperturing it should be possible to generate spin-polarized beams, although with very low efficiency. Our method is also based on selecting only an edge of the beam, although this is done in the radial direction and the efficiency is strongly improved by the vortex-related destructive interference effects. Finally, we note that in our geometry the unavoidable orthogonal magnetic field associated with the azimuthal field gradient generating the dipole forces, which is the main source of problems in the Stern-Gerlach approach to spin-polarized electron separation, is already taken into account and corresponds to the radial magnetic field of the quadrupole or hexapole configuration. So its effect has been already fully considered in our treatment.

---

[1] M. R. Scheinfein, *Optik* **82**, 99 (1989).

[2] J. Verbeeck, H. Tian, and P. Schattschneider, *Nature* **467**, 301 (2010).

- [3] O. Darrigol, *Historical Studies in the Physical Sciences* **15**, 39 (1984).
- [4] H. Batelaan, T. J. Gay, and J. J. Schwendiman, *Phys. Rev. Lett.* **79**, 4517 (1997).
- [5] G. A. Gallup, H. Batelaan, and T. J. Gay, *Phys. Rev. Lett.* **86**, 4508 (2001).
- [6] S. McGregor, R. Bach, and H. Batelaan, *New J. Phys.* **13**, 065018 (2011).